Journal of Inorganic Biochemistry 193 (2019) 94–105

Contents lists available at ScienceDirect

Journal of Inorganic Biochemistry

journal homepage: www.elsevier.com/locate/jinorgbio

Synthesis, characterization and biological evaluation of Co(III) complexes with quinolone drugs

Máté Kozsup[a], Etelka Farkas[a,*], Attila Cs. Bényei[b], Jana Kasparkova[c], Hana Crlikova[c], Viktor Brabec[d], Péter Buglyó[a,*]

[a] Department of Inorganic and Analytical Chemistry, University of Debrecen, H-4032 Debrecen, Egyetem tér 1, Hungary
[b] Department of Physical Chemistry, University of Debrecen, H-4032 Debrecen, Egyetem tér 1, Hungary
[c] Department of Biophysics, Palacky University, Slechtitelu 27, 78371 Olomouc, Czech Republic
[d] Institute of Biophysics, Czech Academy of Sciences, Kralovopolska 135, 61265 Brno, Czech Republic

A B S T R A C T

Nine novel cobalt(III) ternary complexes bearing 4N donor ligands (tris(2-aminoethyl)amine (tren) or tris(2-methylpyridyl)amine (tpa)) and (fluoro)quinolones (quinH) with antibacterial and potential antitumor activity have been synthesized, characterized and screened in various biological assays. The molecular structures of $[Co(tpa)(nal)](PF_6)_2$ (**3**) and $[Co(tpa)(nor)(Co(tpa)(norH)](PF_6)_3(Cl)_2{\cdot}5MeOH$ (**8**) (nal = deprotonated form of nalidixic acid, norH = norfloxacin) with the expected octahedral geometry and (O,O) coordination of the quinolone ligands are also reported. Cyclic voltammetric studies revealed that the 4N donor ligands have much higher effect on the reduction potential of these ternary complexes than the quinolones. Due to the π-back-bonding interaction of the metal ion with the pyridyl-N atoms, the tpa containing compounds demonstrated lower stability and were easier to get reduced in a reversible manner. This character makes them unlikely candidates for development of effective, highly selective hypoxia-activated pro-drug complexes, but this goal might be achieved by substitution of tpa by tren. $[Co(tren)(cip)](PF_6)_2$ (**4**) and $[Co(tpa)(cip)](PF_6)_2$ (**5**) (cip = deprotonated form of ciprofloxacin) showed slightly less antibacterial activity against *Escherichia coli* than free ciprofloxacin (cipH) and they found to have very low toxicity towards both selected cancer (HeLa, MCF 7, MDA-MB-239) and noncancerous (MRC5 pd30) cells. Interaction of **4** and **5** with calf thymus DNA studied by UV–Vis, flow linear dichroism, viscometry and DNA melting indicated the complexes to bind to DNA as intercalators. DNA electrophoresis revealed that, unlike Co(II) complexes, **4** and **5** are not capable of cleaving DNA, but they can inhibit bacterial DNA gyrase **5** being slightly more active than **4**.

1. Introduction

Quinolones (quinH), bearing a 4-oxo-1,4-dihydroquinoline skeleton, are among the most widely used synthetic antibacterial agents and the mechanism of their action is known to rely on the inhibition of the enzymes responsible for DNA replication - topoisomerase II (or DNA gyrase) and topoisomerase IV [1–3]. Nalidixic acid (nalH), as the first representative, was introduced into clinical practice in the early 1960s [4,5]. Its limited activity initiated work on development of structurally related, second, third and fourth generation derivatives with a more enhanced spectrum of antibacterial activity. Very active drugs against aerobic Gram-negative microorganisms, but less active against Gram-positive microorganisms were obtained via the introduction of a fluorine atom in the 6-position of the basic quinolone ring [1–5]. Some of the fluoroquinolone-based antibiotics, e.g. ciprofloxacin, are among the most widely used antibiotics worldwide [5].

Development of new antibiotics, however, is a permanent demand. This is, because, e.g. microbial resistance to antibiotics is a global problem and rapid increases in the number of multidrug resistant bacteria can be registered. To overcome the problem, the introduction of new active compounds against new targets is a continuous task. In this subject, during the past few decades, the suitability of metal complexes of different generations of quinolones as candidates for biological testing in quinolone-resistant microorganisms have been investigated, and a large number of relevant publications, including review articles have been reported [6–9]. Results of various studies suggest that the cell intake route of free quinolone is different from that of quinolone–metal complexes. This supports the suitability of metal complexes as candidates for further biological testing in quinolone resistant microorganisms.

Recently, in addition to their antimicrobial activity, much attention has also been devoted to the cytotoxic properties of quinolones, especially fluoroquinolones [10–19]. For example, some of commonly used antibiotics were found to exhibit significant dose-dependent cytotoxicity against bladder cancer cells [13,14]. Ciprofloxacin has also been shown to affect proliferation of human osteosarcoma cells and leukemic cell lines in vitro [14,15].

In the cancer therapy, selective targeting is also crucial. It is a

* Corresponding authors.
E-mail addresses: efarkas@science.unideb.h (E. Farkas), buglyo@science.unideb.hu (P. Buglyó).

https://doi.org/10.1016/j.jinorgbio.2019.01.005
Received 18 October 2018; Received in revised form 10 January 2019; Accepted 11 January 2019
Available online 21 January 2019
0162-0134/

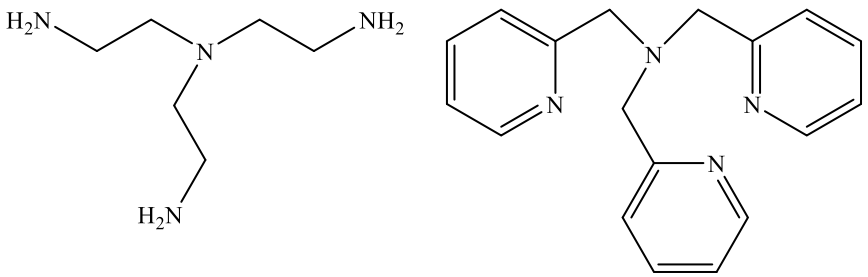

Fig. 1. Structure and abbreviation of the studied 4N donor ligands.

common situation that selectivity and efficiency problems can be associated with some interaction of the drugs during their transportation to the target. To solve the problem, chaperoning of the drug molecule to the site of action in an inactive form and activation of it at the site is one of the known approaches [20–22]. If drug molecules are potential chelating ligands, like the quinolones, their inactivation may be achieved via their chelation to the metal centre of kinetically inert pro-drug complexes. The very significant difference in kinetic lability between the complexes of cobalt(III) and cobalt(II) (the former complexes are very inert, the latters are fairly labile) makes this metal preferred to construct hypoxia selective pro-drug complexes [23]. Although some results can be found related to cobalt(II) complexes of quinolones/fluoroquinolones [11,16,17], any result on relevant cobalt(III) complexes is scarce in the literature. This is the main reason, why synthesis and characterization of cobalt(III) ternary complexes with the involvement of selected quinolones/fluoroquinolones have been performed in the present work. Commonly used tripodal 4N-donor ligands, tris(2-methylpyridyl)amine (tpa) and tris(2-aminoethyl)amine (tren) (Fig. 1) were selected to synthesize chaperons with stabilized +3 oxidation state of the central metal ion, while the coordination sphere was completed via nalidixic acid, ciprofloxacin, norfloxacin, sparfloxacin (spaH) or levofloxacin (levH). The formulae of the used ligands are summarized in Fig. 2 and they are abbreviated as quinH in general throughout this paper.

2. Experimental

2.1. Materials and reagents

$CoCl_2{\cdot}6H_2O$, $NaNO_2$, tris(2-aminoethyl)amine (tren), nalidixic acid, ciprofloxacin, levofloxacin, norfloxacin, sparfloxacin, $NaClO_4$, $NaBF_4$, NH_4PF_6, 96% ethanol and methanol were commercial products from Merck, SigmaAldrich, TCI Chemicals, Acros Organics, Scharlau and Reanal; and used as received. Tris(2-pyridylmethyl)amine (tpa) [24], $Co(tren)(NO_2)_2]Cl$, $[Co(tren)Cl_2]Cl$, $[Co(tpa)(NO_2)_2]Cl$, $[Co(tpa)Cl_2]Cl$ [25] were synthesized and purified according to literature procedures.

2.2. Synthesis of the complexes

2.2.1. $[Co(tren)(lev)](PF_6)_2$ (1)

LevH (115.63 mg, 0.32 mmol) was dissolved in 15 mL 96% ethanol and 1 equiv. 1 M KOH (320 μL) was added. $[Co(tren)Cl_2]Cl$ (100.00 mg, 0.32 mmol), dissolved in 5 mL water, was added and the pH was adjusted to 9, using 1 M KOH. The purple reaction mixture was stirred at 60 °C overnight. The colour of the solution turned deep red and after cooling, NH_4PF_6 (104.38 mg, 0.64 mmol) was added. Orange crystalline solid appeared after few days, by slow evaporation at room temperature. The solid was filtered off and dried in vacuo. Yield: 106.28 mg (39%). ^{1}H NMR (400 MHz, DMSO): δ/ppm = 9.18 (s, 1H, Ar-H); 7.86 (d, 1H, Ar-H); 5.51 (m, 2H, -CH_2); 5.18 (m, 5H, -CH, -NH_2); 4.68 (m, 1H, -NH_2); 4.34 (m, 1H, -NH_2); 3.54 (m, 2H, tren-H); 3.33 (m, 8H, tren-H, -CH_2); 3.18 (t, 2H, tren-H); 2.92 (m, 3H, -CH_2); 2.73 (m, 5H, tren-H); 2.27 (s, 3H, -CH_3) 1.47 (d, 3H, -CH_3). IR (KBr)/cm^{-1}: 3434, 3221, 3120, 1636, 1520, 1472, 1281, 843, 558. Anal. Required for $C_{24}H_{37}CoF_{13}N_7O_4P_2$: C, 33.70, H, 4.36, N, 11.46%. Found: C, 33.77, H, 4.63N, 11.03%. MS (ESI, positive ion): m/z: 282.608 ($[Co(tren)(lev)]^{2+}$).

2.2.2. $[Co(tren)(nal)](PF_6)_2$ (2)

The synthesis was similar to that of **1**, using nalH (74.32 mg, 0.32 mmol). The complex was isolated as pink crystalline solid. Yield: 104.15 mg (45%). ^{1}H NMR (400 MHz, DMSO): δ/ppm = 9.49 (s, 1H, Ar-H); 8.80 (d, 1H, Ar-H); 7.74 (d, 1H, Ar-H); 5.69 (m, 2H, -NH_2); 5.34–5.21 (m, 4H, -NH_2); 4.79 (q, 2H, -CH_2); 3.36 (m, 4H, tren-H); 3.13 (m, 2H, tren-H); 3.02 (m, 2H, tren-H); 2.76 (m, 5H, tren-H, -CH_3); 2.63 (m, 2H, tren-H); 1.43 (t, 3H, N-CH_2-*CH_3*). IR (KBr)/cm^{-1}: 3339, 3281, 3058, 1611, 1565, 1523, 1498, 1452, 1262, 835. Anal. Required for $C_{18}H_{29}CoF_{12}N_6O_3P_2$: C, 29.77, H, 4.02, N, 11.57%. Found: C, 29.37, H, 4.05, N, 11.48%. MS (ESI, positive ion): m/z: 581.123 ($[Co(tren)(nal)](PF_6)^+$).

2.2.3. $[Co(tpa)(nal)](PF_6)_2$ (3)

The synthesis was similar to that of **1**, using $[Co(tpa)Cl_2]Cl$ (145.81 mg, 0.32 mmol) and nalH (74.32 mg, 0.32 mmol). The complex was isolated as a deep red crystalline solid. Yield: 89.46 mg (32%). ^{1}H NMR (400 MHz, DMSO): δ/ppm = 9.56 (s, 1H, Ar-H); 9.14 (d, 1H, py-H); 9.00 (d, 1H, py-H); 8.43 (m, 1H, Ar-H); 8.24 (m, 1H, py-H); 8.10 (m, 2H, py-H); 8.03 (m, 1H, py-H); 7.78 (m, 3H, py-H); 7.63 (m, 3H, py-H, Ar-H); 7.42 (m, 1H, py-H); 5.79 (d, 2H, tpa-CH_2); 5.31 (s, 2H, tpa-CH_2); 5.13 (d, 2H, tpa-CH_2); 4.71 (q, 2H, Nal-CH_2); 2.69 (s, 3H, -CH_3); 1.38 (t, 3H, -CH_3). IR (KBr)/cm^{-1}: 3420, 3087, 2977, 1724, 1651, 1488, 1449, 1287, 1258, 803, 558. Anal. Required for $C_{30}H_{29}CoF_{12}N_6O_3P_2$: C, 41.39, H, 3.36, N, 9.65%. Found: C, 41.67, H, 3.35 N, 9.74%. MS (ESI, positive ion): m/z: 725.126 ($[Co(tpa)(nal)](PF_6)^+$).

2.2.4. $[Co(tren)(cip)](PF_6)_2{\cdot}1H_2O$ (4)

The synthesis was similar to (**1**), using cipH (106.03 mg, 0.32 mmol), without adjusting the pH to 9. The reaction mixture was stirred at 80 °C. The complex was isolated as a pink crystalline solid. Yield: 98.75 mg (37%). ^{1}H NMR (400 MHz, DMSO): δ/ppm = 8.93 (s, 1H, Ar-H); 8.13 (d, 1H, Ar-H); 7.61 (d, 1H, Ar-H); 5.46 (m, 2H, -NH_2); 5.11 (m, 4H, -NH_2); 4.01 (m, 1H, -CH); 3.55 (m, 2H, tren-H); 3.28 (m, 5H, tren-H, -CH_2); 3.17 (m, 2H, tren-H); 2.93 (m, 6H, tren-H, -CH_2); 2.72 (m, 5H, tren-H, -CH_2); 1.44 (m, 2H, -CH_2 cp); 1.10 (m, 2H, -CH_2 cp). IR (KBr)/cm^{-1}: 3327, 3132, 1638, 1521, 1476, 1260, 844, 558. Anal. Required for $C_{23}H_{37}CoF_{13}N_7O_4P_2$: C, 32.75, H, 4.42, N, 11.62%. Found: C, 32.90, H, 4.28, N, 11.57%. MS (ESI, positive ion): m/z: 680.175 ($[Co(tren)(cip)](PF_6)^+$).

2.2.5. $[Co(tpa)(cip)](PF_6)_2{\cdot}2H_2O$ (5)

The synthesis was similar to (**1**), using $Co(tpa)Cl_2]Cl$ (145.81 mg, 0.32 mmol) and cipH (106.03 mg, 0.32 mmol), without adjusting the pH to 9. The reaction mixture was stirred at 50 °C. The complex was isolated as an orange crystalline solid. Yield: 112.37 mg (35%). ^{1}H NMR

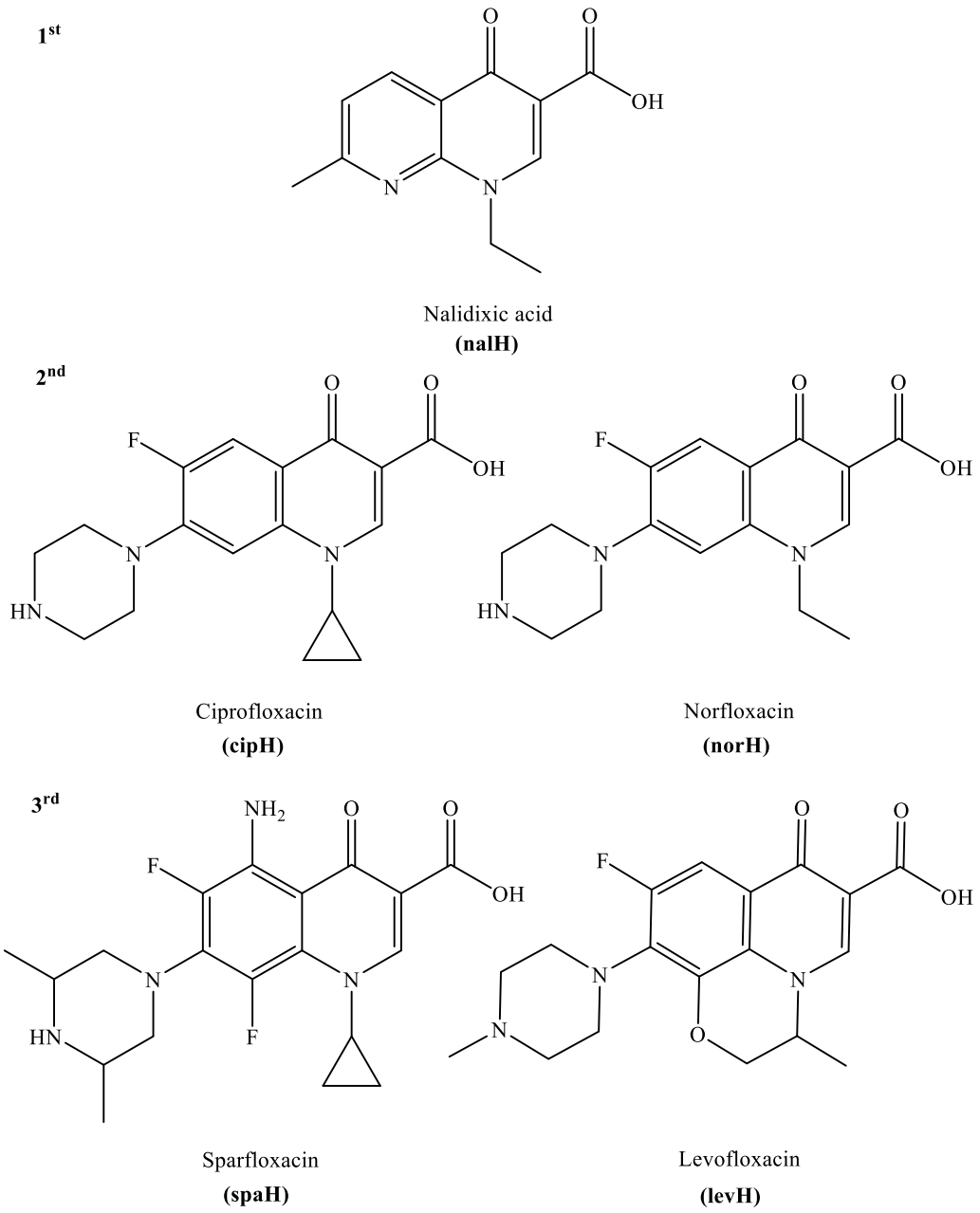

Fig. 2. Structure and abbreviation of the studied 1st, 2nd and 3rd generation quinolones.

(400 MHz, DMSO): δ/ppm = 9.39 (d, 1H, py-H); 9.15 (d, 1H, py-H); 9.06 (m, 1H, Ar-H); 8.85 (s, 1H, Ar-H); 8.71 (s, 1H, Ar-H); 8.37 (m, 1H, py-H); 8.31 (m, 1H, py-H); 8.17 (m, 1H, py-H); 8.01 (m, 1H, py-H); 7.87 (m, 1H, py-H); 7.80 (m, 1H, py-H); 7.61–7.42 (m, 4H, py-H); 5.79 (d, 0.67H, tpa-CH_2 isomer B); 5.45 (d, 1.33H, tpa-CH_2 isomer A); 5.31 (s, 0.67H, tpa-CH_2 isomer B); 5.25 (s, 1.33H, tpa-CH_2 isomer A); 5.09 (d, 0.67H, tpa-CH_2 isomer B); 4.91 (d, 1.33H, tpa-CH_2 isomer A); 4.02 (m, 1H, -CH); 3.66 (m, 2H, -CH_2); 3.49 (m, 2H, -CH_2); 3.41 (m, 2H, -CH_2); 3.32 (m, 2H, -CH_2); 1.35 (m, 2H, -CH_2 cp); 1.19 (m, 2H, -CH_2 cp). IR (KBr)/cm^{-1}: 3422, 3249, 3119, 1639, 1524, 1471, 1272, 841, 558. Anal. Required for $C_{35}H_{39}CoF_{13}N_7O_5P_2$: C, 41.80, H, 3.91, N, 9.70%. Found: C, 41.55, H, 3.92, N, 9.82%. MS (ESI, positive ion): m/z: 339.605 ($[Co(tpa)(cip)]^{2+}$).

2.2.6. [Co(tren)(spa)](PF$_6$)(Cl)·2H$_2$O (6)

NaOH (12.80 mg, 0.32 mmol) was dissolved is 12 mL methanol. spaH (125.57 mg, 0.32 mmol) was added, giving a yellow solution. [Co(tren)Cl_2]Cl (100.00 mg, 0.32 mmol) was added and the reaction mixture was stirred at 60 °C overnight. The red solution was kept at 4 °C for one day and NH_4PF_6 (104.32 mg, 0.64 mmol) was added. Orange crystalline solid appeared in one day. The solid was filtered off and dried in vacuo. Yield: 123.55 mg (48%). ^{1}H NMR (400 MHz, D_2O): δ/ppm = 8.98 (s, 1H, Ar-H); 4.23 (m, 1H, -CH); 3.72 (m, 2H, tren-H); 3.57 (m, 6H, tren-H, -CH_2, -CH); 3.28 (m, 6H, tren-H, -CH_2, -CH); 2.97 (m, 2H, tren-H); 2.88 (m, 2H, tren-H); 1.32 (m, 6H, -CH_3); 1.15 (m, 4H, -CH_2 cp). ^{1}H NMR (400 MHz, DMSO): δ/ppm = 8.77 (s, 1H, Ar-H); 6.55 (m, 2H, -NH_2 spa); 5.72 (m, 2H, -NH_2 tren); 5.62 (m, 2H, -NH_2 tren); 5.52 (m, 2H, -NH_2 tren); 4.09 (m, 1H, -CH); 3.30 (m, 2H, tren-H); 3,17 (m, 6H, tren-H, -CH_2, -CH); 2,97 (m, 6H, tren-H, -CH_2, -CH); 2.87 (m, 2H, tren-H); 2.66 (m, 2H, tren-H); 1.22 (m, 3H, -CH_3); 1.09 (m, 7H, -CH_2 cp, -CH_3). IR (KBr)/cm^{-1}: 3404, 3328, 3211, 3091, 1640, 1525, 1433, 1298, 1182, 1030, 845, 559. Anal. Required for $C_{25}H_{43}CoF_8N_8O_5PCl$: C, 36.93, H, 5.33, N, 13.78%. Found: C, 36.52, H, 5.43, N, 13.33%. MS (ESI, positive ion): m/z: 298.120 ($[Co(tren)(spa)]^{2+}$).

2.2.7. [Co(tpa)(norH)](BF4)3·3H2O (7)

The synthesis was similar to (**6**), using $[Co(tpa)Cl_2]Cl$ (145.81 mg, 0.32 mmol), norH (102.19 mg, 0.32 mmol) and $NaBF_4$ (70.27 mg, 0.64 mmol) instead of NH_4PF_6. The complex was isolated as a pink crystalline solid. Yield: 61.79 mg (20%). ^{1}H NMR (400 MHz, DMSO): δ/ppm = 9.36 (m, 1H, py-H); 9.31 (s, 1H, Ar-H); 9.02 (s, 1H, Ar-H); 8.34 (d, 2H, py-H); 8.13 (t, 2H, py-H); 8.04 (m, 1H, py-H); 7.87 (m, 1H, py-H); 7.80 (m, 2H, py-H); 7.47 (t, 2H, py-H); 7.41 (m, 2H, py-H, Ar-H); 5.49 (d, 2H, tpa-CH_2); 5.24 (s, 2H, tpa-CH_2) 4.94 (d, 2H, tpa-CH_2); 4.75 (q, 2H, nor-CH_2); 3.63 (m, 2H, nor-CH_2); 3.33 (m, 6H, nor-CH_2); 1.43 (t, 3H, –CH_3). IR (KBr)/cm^{-1}: 3434, 1640, 1525, 1472, 1273, 1095, 771, 625. Anal. Required for $C_{34}H_{42}B_3CoF_{13}N_7O_6$: C, 42.29, H, 4.16, N, 9.86%. Found: C, 42.65, H, 4.35, N, 10.27%. MS (ESI, positive ion): m/z: 333.606 ($[Co(tpa)(nor)]^{2+}$).

2.2.8. [Co(tren)(nor)](PF6)2 (8)

The synthesis was similar to (**6**), using $[Co(tren)Cl_2]Cl$ (125.00 mg, 0.40 mmol), norH (127.74 mg, 0.40 mmol). The complex was isolated as a pink crystalline solid. Yield: 95.44 mg (29%). ^{1}H NMR (400 MHz, D_2O): δ/ppm = 9.08 (s, 1H, Ar-H); 8.23 (d, 1H, Ar-H); 7.34 (d, 1H, Ar-H); 4.65 (q, 2H, -CH_2); 3.83 (m, 2H, tren-H); 3.55 (m, 2H, tren-H); 3.37 (m, 6H, tren-H, -CH_2); 3.18 (m, 2H, tren-H); 3.06 (m, 4H, -CH_2); 2.97 (m, 2H, tren-H); 2.90 (m, 2H, tren-H); 1.59 (t, 3H, -CH_3). ^{1}H NMR (400 MHz, DMSO): δ/ppm = 9.16 (s, 1H, Ar-H); 8.18 (d, 1H, Ar-H); 7.26 (d, 1H, Ar-H); 5.49 (m, 2H, -NH_2); 5.25 (m, 4H, -NH_2); 4.75 (q, 2H, -CH_2); 3.55 (m, 4H, tren-H); 3.17 (m, 2H, tren-H); 3.10 (m, 6H, tren-H, -CH_2); 2.91 (m, 3H, tren-H); 2.73 (m, 5H, -CH_2, tren-H); 1.42 (t, 3H, -CH_3). IR (KBr)/cm^{-1}: 3445, 3277, 1637, 1481, 1256, 1092, 845, 625, 558. Anal. Required for $C_{22}H_{39}P_2CoF_{13}N_7O_5$: C, 31.11, H, 4.63, N, 11.54%. Found: C, 30.96, H, 4.85, N, 11.42%. MS (ESI, positive ion): m/z: 261.603 ($[Co(tren)(nor)]^{2+}$).

2.2.9. [Co(tpa)(lev)](ClO4)2·3H2O (9)

$[Co(tpa)Cl_2]Cl$ (72.91 mg, 0.16 mmol) and levH (57.82 mg, 0.16 mmol) were dissolved in 10 mL water and NaOH (6.4 mg, 0.16 mmol) was added. The reaction mixture was stirred at 60 °C overnight and it was cooled at 4 °C for one day. Some solid was filtered off using cotton wool, and $NaClO_4$ (39.18 mg, 0.32 mmol) was added. The complex was isolated as a red crystalline solid. The crystals were filtered off and dried in vacuo. Yield: 59.15 mg (38%). ^{1}H NMR (400 MHz, D_2O): δ/ppm = 9.36 (d, 1H, py-H isomer A); 9.19 (d, 1H, py-H isomer B); 9.06 (s, 1H, Ar-H isomer A); 8.91 (s, 1H, Ar-H isomer B); 8.60 (d, 1H, Ar-H isomer A); 8.45 (d, 2H, py-H); 8.31 (m, 2H, Ar-H isomer B, py-H); 8.09–7.99 (m, 4H, py-H); 7.98–7.88 (m, 2H, py-H); 7.79–7.66 (m, 7H, py-H); 7.53 (m, 2H, py-H); 7.44 (m, 2H, py-H); 7.31 (m, 2H, py-H); 5.78–5.60 (m, 1H, tpa-CH_2); 5.05 (m, 1H, tpa-CH_2); 4.92–4.81 (m, 9H, tpa-CH_2, lev-CH_2); 4.63 (d, 1H, tpa-CH_2); 4.53–4.43 (m, 3H, tpa-CH_2); 4.33 (d, 1H, tpa-CH_2); 3.58 (t, 4H, -CH_2 isomer A); 3.38 (t, 4H, -CH_2 isomer B); 2.84 (t, 4H, -CH_2 isomer A); 2.72 (t, 4H, -CH_2 isomer B); 2.47 (s, 3H, -CH_3 isomer A); 2.40 (s, 3H, -CH_3 isomer B); 1.58 (d, 3H, -CH_3 isomer A); 1.50 (d, 3H, -CH_3 isomer B). IR (KBr)/cm^{-1}: 3439, 1633, 1519, 1448, 1272, 1094, 624. Anal. Required for $C_{36}H_{43}Cl_2CoFN_7O_{15}$: C, 44.92, H, 4.50, N, 10.19%. Found: C, 44.65, H, 4.15, N, 10.14%. MS (ESI, positive ion): m/z: 354.612 ($[Co(tpa)(lev)]^{2+}$).

2.3. NMR, IR and Electrospray Ionization Mass Spectrometric (ESI-MS) measurements

NMR measurements were carried out using Bruker Avance 400 NMR spectrometer at room temperature on samples prepared in D_2O or/and d^6-DMSO. Calibration was performed using the signals of the solvents (2.50 ppm for DMSO and 4.79 ppm for D_2O). For ^{19}F NMR 10 mM NaF was used as a standard. IR spectra as KBr pellets were recorded on a Perkin Elmer FTIR Paragon 1000 PC instrument at the Department of Organic Chemistry, University of Debrecen. ESI-TOF MS measurements in the positive mode were carried out on a Bruker micrOTOF-Q instrument at the Department of Applied Chemistry, University of Debrecen. The concentration of the samples was 10 μg/mL and the solvent was water or methanol. The instrument was equipped with an electrospray ion source, where the voltage was 4 kV. The drying gas was N_2. The flow rate was 4 L/min and the drying temperature was 200 °C. The spectrums were recorded by means of a digitizer at a sampling rate of 2 GHz. The mass spectra were calibrated externally, using the exact masses of clusters $[(NaTFA)_n + Na]^+$ generated from the electrosprayed solution of sodium-trifluoroacetate (NaTFA). The spectra were evaluated with DataAnalysis 3.4 software from Bruker. The samples were introduced directly into the ESI with a syringe pump at a flow rate of 3 μL/min.

2.4. Crystal structure analysis

Single crystals of **3** or **8** were grown by the slow evaporation of methanolic solutions. X-ray diffraction data were collected at 298 K using a Bruker-Nonius MACH3 diffractometer equipped with a point detector for **3** while at 100 K using a Bruker-D8 Venture diffractometer equipped with INCOATEC IμS 3.0 dual (Cu and Mo) sealed tube microsources and Photon II Charge-integrating Pixel Array detector for **8**. In both cases Mo Kα (λ = 0.7107 Å) radiation was applied. Crystals of **3** were very weakly diffracting. In case of structure **8** data collection and integration was performed using the APEX3 software Data reduction and multi-scan absorption correction was applied. The structure could be solved using direct methods and refined on F2 using SHELXL [26] program incorporated into the WINGX suite [27]. Refinement was performed anisotropically for all non-hydrogen atoms. Hydrogen atoms were placed into geometric positions. In structure **3** one of the counter ions of PF_6^- is distributed among two positions with occupancy of 50–50%. In structure **8** two cobalt complexes were found in the asymmetric unit. Ordered and disordered solvent methanol molecules, disordered PF_6^- over two positions in general position as well as PF_6^- in special position were found. Moreover, the structure of **8** contains one chloride ion and partial protonation of one of the amine moieties (most likely at the piperazine ring) is suggested as well. Tables were extracted from the edited CIF file using publCIF [28]. The PLATON program [29] was used for crystallographic calculations. Further information on the data collection and refinement for the respective compounds can be found in Table S1. CCDC numbers for structures **3** and **8** are 1866883 and 1866884, respectively.

2.5. Cyclic voltammetric (CV) studies

Cyclic voltammetric experiments were performed within the voltage range +600 to −1000 mV, at room temperature in the solution of H_2O:MeOH = 1:1, using a Metrohm 746–747 VA Trace Analyser equipped with a three-electrode system, which consists of a Ag/AgCl/3M KNO_3 reference electrode ($E_{1/2}$ = 209 mV vs. NHE), a platinum wire auxiliary electrode (ALS Co. Japan), and a glassy carbon (CHI104) working electrode. Aqueous solution of $K_3[Fe(CN)_6]$ was used to calibrate the system ($E_{1/2}$ = 0.458 V versus NHE in 0.50 M KCl) [30]. The samples were degassed before the measurements using argon. The concentration of the complexes was 1 mM, the potential sweep rates were 200 mV s^{-1} during the determination of the redox potentials. In all cases, KNO_3 (0.20 M) was used as a supporting electrolyte.

2.6. Biological studies

Commercial reagent grade chemicals, solvents, and reagents for the preparation of solutions for biological work were used as received from commercial suppliers without further purification. Calf thymus (ct) DNA (42% G + C, mean molecular mass ca. 20,000 kDa) was from Sigma (Prague, Czech Republic). The plasmids pBR322 (4361 bp) was isolated according to standard procedures. Agarose was from Merck

KgaA (Darmstadt, Germany). 3-(4,5-dimethylthiazol-2-yl)-2,5-diphenyltetrazolium bromide (MTT) was obtained from Calbiochem (Darmstadt, Germany). The selected complexes **4** and **5** were freshly dissolved in water to the concentration of 2 mM. (Due to the inertness of the cobalt(III) complexes, any dissociation of the coordinated ligands from the complexes was not detected.) Ciprofloxacin was always freshly dissolved in 0.04 M NaOH to 30 mM. For the experiments, the stock solutions were diluted by 0.01 M Tris.Cl buffer (pH 7.4) to appropriate concentrations.

The human cervical carcinoma HeLa cells and human breast cancer MCF-7 cells were kindly supplied by Professor B. Keppler, University of Vienna (Austria). Highly invasive breast carcinoma MDA-MB-231 cells and human MRC-5 pd30 cells derived from normal lung tissue were purchased from the European collection of authenticated cell cultures (ECACC) (Salisbury, UK). The cells were grown in Dulbecco's Modified Eagle Medium (DMEM) (high glucose 4.5 gL^{-1}, fetal bovine serum (PAA)) supplemented with gentamycin (50 μg/mL, Serva) and 10% heat inactivated PAA, with (MDA-MB-231 and MRC-5 pd30 cells) or without (HeLa and MCF-7 cells) 1% non-essential amino acids (Sigma-Aldrich, Prague, Czech Republic). The cells were cultured in a humidified incubator at 37 °C in a 5% CO_2 atmosphere and subcultured 2–3 times a week with an appropriate plating density.

Escherichia coli (*E. coli*, CCM 7929) was obtained from the Czech Collection of Microorganisms (CCM), Masaryk University, Faculty of Science, Brno, Czech Republic as a freeze-dried pellet. The cells were rehydrated and propagated on Luria broth (LB) agar plates according to the supplier protocol. Microbiological experiments were performed under standard sterile conditions.

Cytotoxicities against human cancer and noncancerous cells were evaluated by using an assay based on the tetrazolium compound MTT. The cells were seeded in 96-well tissue culture plates at a density of 5000 HeLa cells/well in 100 μL of medium. After overnight incubation at 37 °C in a 5% CO_2 humidified atmosphere, the cells were treated with the compounds tested in this work in a final volume of 200 μL/well. After 72 h of incubation, 10 μL of a freshly diluted MTT (Calbiochem, Darmstadt, Germany) solution (2.5 mg/mL in phosphate buffered saline (PBS)) was added to each well and the plates were incubated at 25 °C in a humidified 5% CO_2 atmosphere for 4 h. At the end of the incubation, the medium was removed and the formazan product was dissolved in 100 μL of DMSO. The cell viability was evaluated by measurement of the absorbance at 570 nm (reference 620 nm), using an Absorbance Reader (SUNRISE TECAN, Schoeller). All experiments were made in triplicate. The collected values were converted to the percentage of control (% cell survival). Cytotoxic effects were expressed as IC_{50} values calculated from curves constructed by plotting cell survival (%) versus drug concentration (μM) (IC_{50} = concentration of the agent inhibiting cell growth by 50%).

Microtitre broth dilution method was assessed to determine the susceptibility of *E. coli* bacteria to compounds tested in this work. Briefly, overnight grown bacterial culture (carried out in LB at 35 °C) were diluted with fresh LB medium to a final optical density of 0.02, measured at 600 nm. From these cell suspensions, 100 μL aliquots were mixed in the wells of 96-wells polystyrene plates with 100 μL of fresh LB supplemented with the compounds under study, previously serially diluted (1:2) from stock solutions of each compound. At certain times of incubation at 37 °C, the OD_{600} of the cultures were measured using an Absorbance microplate reader (SUNRISE TECAN, Schoeller). The minimum inhibitory concentration (MIC) values, expressed in μM, were estimated by fitting the OD_{600} mean values determined after 24 h of incubation at 37 °C with a Gompertz modified equation as described before [31]. The data were obtained from two independently prepared assays.

UV–vis absorption measurements. UV–vis spectra were recorded at 25 °C on a Varian Cary 4000 UV–vis spectrophotometer in 0.01 M Tris buffer (pH 7.4) by using quartz cells with a path length of 1 cm.

The melting curves of ct DNA at the concentration of 32 μg/mL (0.1 mM in terms of nucleotide content) were recorded with Varian Cary 4000 UV–vis spectrophotometer equipped with a thermoelectrically controlled cell holder and quartz cells with a path length of 1 cm by measuring the absorbance at 260 nm in the medium containing 0.01 M Tris.Cl, pH 7.4. The value of melting temperature (T_m) was determined as the temperature corresponding to a maximum on the first-derivative profile of the melting curves.

Flow linear dichroism (LD) spectra were collected by using a flow Couette cell in a Jasco J-720 spectropolarimeter adapted for LD measurements. The flow cell consists of a fixed outer cylinder and a rotating solid quartz inner cylinder, separated by a gap of 0.5 mm, giving a total path length of 1 mm. LD spectra of ct DNA at the concentration of 0.2 mM were recorded at 25 °C in 0.01 M Tris.Cl, pH 7.4.

The relative viscosity of the solutions of ct DNA (150 μg/mL) in the presence or absence of **4** and **5** was measured in 0.01 M $NaClO_4$ at 37 °C by AMVn Automated Micro Viscometer, (Anton Paar GmbH, Austria) in a 1.6 mm capillary tube.

Native agarose electrophoresis was used to assess the ability of **4** and **5** to cleave DNA. This assay monitors the extent of single strand brakes in DNA as a function of the conversion of supercoiled pBR322 DNA into nicked form (OC). pBR322 (0.5 μg) was incubated with various concentrations of **4** or **5** in a reaction volume of 10 μL containing the 0.01 M Tris buffer (pH 7.4) at 37 °C for 45 min. Samples were then resolved by gel electrophoresis on a 1% agarose gel in TAE buffer (40 mM Tris acetate, 1 mM EDTA pH 8.3). Gels were stained with ethidium bromide and photographed under UV light.

Bacterial gyrase activity was assessed by measuring the decatenation of kinetoplast DNA using the Gyrase Assay Kit (TopoGen, Port Orange, Florida). Kinetoplast DNA (0.2 mM) was preincubated with **4** or **5** in Tris.Cl buffer, pH 7.4 at 37 °C for 30 min. The decatenation assays were performed using *E. coli* bacterial DNA gyrase (TopoGen) according manufacturers protocol. After 30 min of incubation with the enzyme at 37 °C, the reaction was terminated with 10% sodium dodecyl sulfate (SDS), followed by proteinase K treatment (0.3 mg/mL), and phenol/chloroform extraction and separated in 1% agarose gel at 4 Vcm^{-1} at room temperature. The reaction products were stained by ethidium bromide, visualized under ultraviolet light and photographed.

3. Results and discussion

Stochiometric amount of $[Co(4N)Cl_2]Cl$ (4N = tren or tpa) precursor and one of the different types of quinolone/fluoroquinolone bioligands were reacted in polar solvent (EtOH for **1–5**, MeOH for **6–8** and water for **9**) in the presence of one equivalent base at 60 °C overnight. Coloured crystalline solids appeared in few days at room temperature, by adding bulky anion (PF_6^-, BF_4^- or ClO_4^-) to the reaction mixture. In some cases (**1–5**), slow evaporation of the solution at room temperature afforded the complexes. The novel compounds were air stable crystalline solids and soluble in polar solvents, (MeOH, DMSO) and at higher temperature, or in low concentration, in water as well. ^1H NMR spectra of the complexes showed the expected resonance signals. A representative spectrum of **8** is presented in Fig. 3.

In the spectra of the $[Co(tren)(quin)](X)_n$ (X = PF_6^-, BF_4^- or ClO_4^-) complexes the signals of the -CH_2 groups of tren appear in the range of 3.6–2.6 ppm. Therefore, most of the samples were prepared in d^6-DMSO and in this way the signals of the -NH_2 groups also appeared at around 5.5 ppm. For these products, the assignation of the signals of the different groups of the two ligands was simple, because of the aliphatic character of the tren, unlike the quinH ligands with mostly aromatic protons. The assignation was more difficult for the analogous complexes of tpa due to the presence of the three pyridyl arms therefore COSY measurements were also carried out. As an example, COSY spectrum of the aromatic region of **3** is shown in Fig. 4.

In the ^1H NMR spectra of **3** and **7**, the -CH_2 groups of the tpa ligand showed two doublets and one singlet. This indicates that, two -CH_2 groups seem similar to each other, and the coupling of these protons

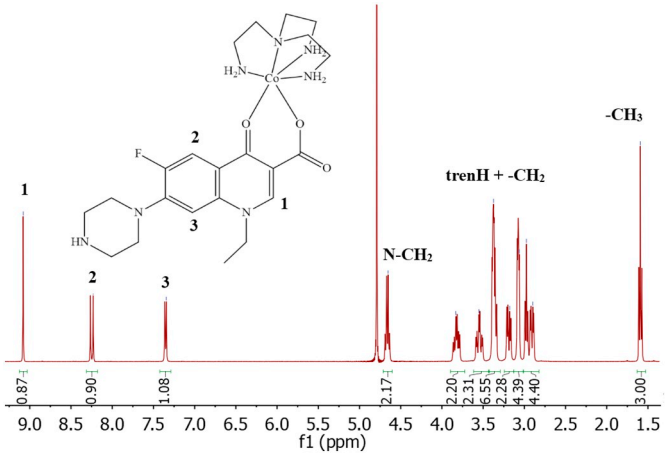

Fig. 3. ^{1}H NMR spectrum of [Co(tren)(nor)](PF$_6$)$_2$ (**8**) in D$_2$O.

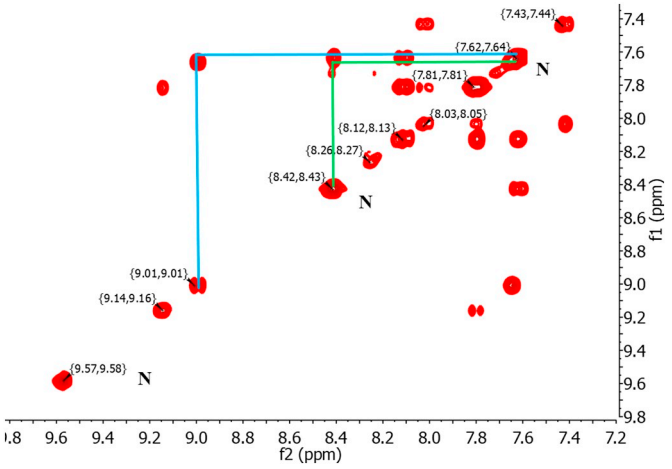

Fig. 4. Aromatic region of the COSY spectrum of [Co(tpa)(nal)](PF$_6$)$_2$ (**3**) in d^6-DMSO.

resulted in doublets in the spectrum. For **5** and **9** the ^{1}H NMR spectra showed the mixture of two isomers. The isomerisation was detected only for the aliphatic tpa protons, all of the signals of the other H-atoms were close enough to each other to give one peak in the spectrum for **5**. Based on the relative intensity of the aliphatic tpa protons, the ratio of the isomers for **5** was found to be 2:1. For **9**, the intensity of the signals of the two isomers were identical, indicating 1:1 ratio of the isomers.

Complexation resulted in upfield shifts (0.08–0.35 ppm) of the aromatic protons of the bioligands in tren analogs, compared these resonances to the free ligands. The tendency was the same for the tpa complexes, but due to the isomeration and the disturbing effect of pyridyl hydrogens, the exact shift values could not be identified.

Complex **8** was crystallized with different counterions (PF_6^-, BF_4^- or ClO_4^-). The ^{1}H NMR spectra of these complexes showed identical chemical shifts, regardless of the counterion. Since spaH contains one -NH$_2$ group next to the coordinating oxo-group in chelating position beside (O,O), (N,O) coordination of this ligand is also possible. Unfortunately the ^{1}H NMR spectra did not provide information about the binding mode therefore ^{19}F NMR measurements were also carried out. Since norH, cipH and levH also have fluorine substituent in position 6, these ligands and their cobalt complexes have also been studied for comparison. The NMR behaviour was checked first by the comparison of the fluorine signals of the fully deprotonated free ligands. In all the cases the signals showed a downfield shift by 1.4–4.5 ppm indicating that in spaH the amino group has no influence on the change of the above signal upon deprotonation of the ligand. In all the cobalt

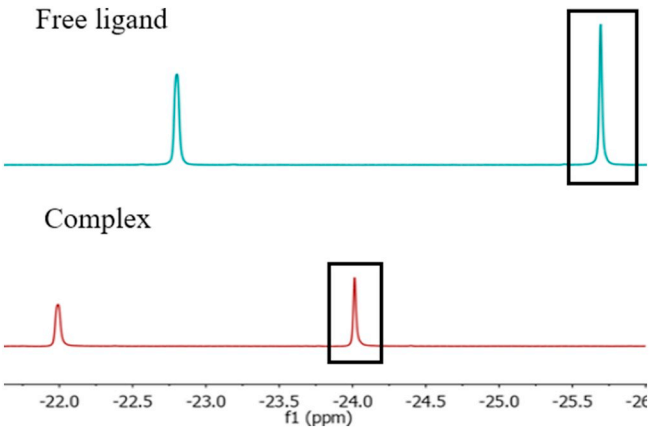

Fig. 5. ^{19}F NMR spectra of spaH and [Co(tren)(spa)](PF$_6$)$_2$ (**6**) in d^6-DMSO. Signals of the fluorine substituents in position 6 are framed.

complexes, the F resonance appeared around 0 ppm, except for **6** (having another F substituent in position 8), where in the spectrum two signals at −20 ppm and −25 ppm could be identified (Fig. 5). The latter peak belongs to the requested F substituent. [32]

Comparing the ^{19}F NMR spectra of the free ligands with those of the corresponding [Co(tren)(quin)]$^{2+}$ complexes, the coordination resulted in upfield shift of the F signals in every case. The extent of the shift was in the range 0.98–1.68 ppm even for **6** too, providing further strong support for the absence of the amino group from coordination (Fig. 6). Similar behaviour of spaH with (O,O) coordination was also found in other reported Co(II) complexes [33,34].

Since the studied tren complexes were PF_6^- salts, the signals of these anions also appeared in the spectra of the complexes at around 50 ppm. The ratio of these signals to those of the substituent F were 12:1 in all the cases, proving that the complexes were crystallized with two PF_6^- anions. The only exception was **6**, where this value was 6:1, indicating one PF_6^- only.

ESI-MS analysis in the positive mode provided further proof for the identity of the complexes. In the mass spectra of all products, the peaks, belonging to the [Co(4N)(quin)]$^{2+}$ or [Co(4N)(quin)](PF$_6$)$^+$ ions, were appeared. Under ESI-MS conditions neither the ligands nor the PF_6^- anions for **2**, **3**, **4** dissociate completely. All the mass spectra displayed the correct isotopic pattern (Fig. S1).

The identity of the complexes was further proved using CHN measurements. The experimental data are in good agreement with the calculated ones. For **6**, the CHN data confirmed that the complex was crystallized with one PF_6^- and one Cl^-. The result shows that, most of the complexes (**4**–**9**) also have water molecules in their crystal structure.

The significant functional groups of the novel complexes, involved in the coordination, were also studied by IR. There were two strong absorption bands in the spectrum of the quinH ligands at ~1720 cm^{-1}, and ~1630 cm^{-1} assigned to υ(COOH) and υ(C=O) stretching vibrations. On comparison of these IR wavenumbers, the band at ~1720 cm^{-1} has been replaced by two strong characteristic bands at ~1470 cm^{-1} and ~1270 cm^{-1}, as υ(O–C–O) asymmetric and symmetric stretching vibrations, whereas υ(C=O) is shifted by max. 10–20 cm^{-1} upon bonding. These changes indicated that the ligands are bound to the cobalt centre via these two oxygen atoms. [35–38]

The molecular structure of some of these novel ternary complexes were also assessed by single crystal analysis. The appropriate details of data collection and refinement for the complexes **3** and **8** can be found in Table S1. The obtained structures together with key bond length values for **3** and **8** can be seen in Figs. 7 and 8. The structures show the expected octahedral, monomeric structures consisting of one 4N donor ligand and one quinolone ligand coordinating to the central metal ion. In both cases the quinolones are bound via the carbonyl and the phenolate O donor atoms. Comparing these structures with those six hits

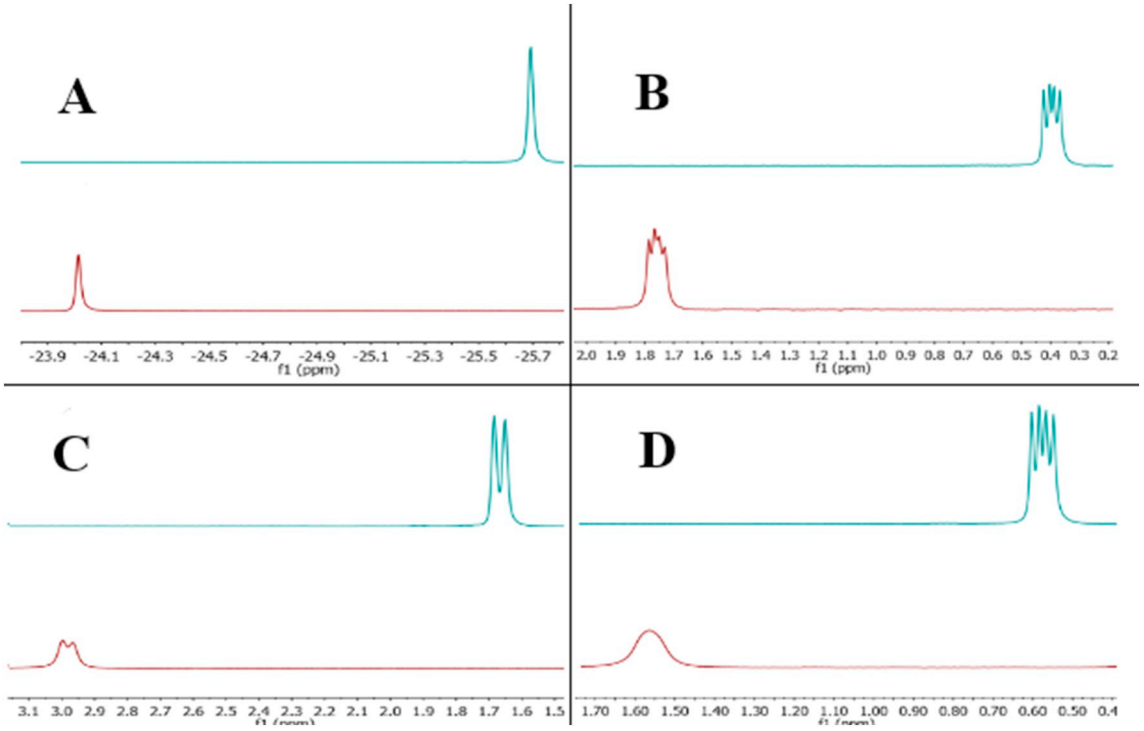

Fig. 6. ^{19}F NMR spectra of the free ligands (above) and their Co(III)-tren complexes (below) in d^6-DMSO (A: spaH and [Co(tren)(spa)](PF_6)Cl, B: cipH and [Co(tren)(cip)]$(PF_6)_2{\cdot}1H_2O$ C: levH and [Co(tren)(lev)]$(PF_6)_2$ D: norH and [Co(tren)(nor)]$(PF_6)_2$).

available in the CCDC for similar Co(II) complexes, it is worth noting that in the previously published complexes where beside the quinolone ligands only one (N,N) donor molecule (e.g. 2,2′-bipyridine or 1,10-phenantroline) is *co*-present dimeric or carboxylate bridged polymeric structures were revealed [39–43]. For the new complexes, **3** and **8**, the presence of the 4N donor tren or tpa successfully hinders the aggregation of the monomeric units. Furthermore, in the structure of **8** two octahedral cobalt complexes were found in the asymmetric unit. Ordered and disordered solvent methanol molecules, disordered PF_6^- over two positions in general position as well as PF_6^- in special position were found. Interestingly, the structure of the obtained single crystal also contains one chloride ion therefore partial protonation of one of the amine moieties is suggested as well.

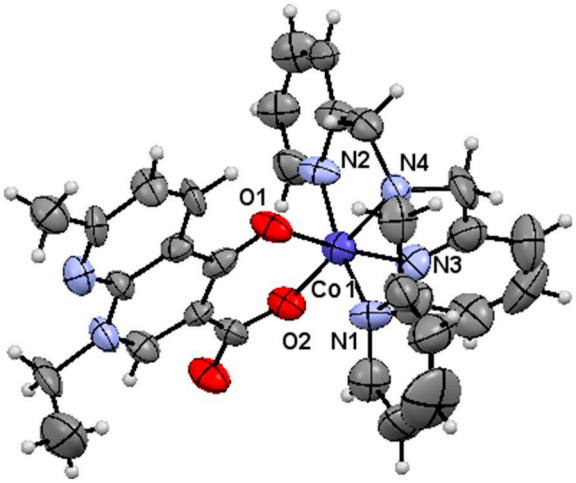

Fig. 7. ORTEP view of [Co(tpa)(nal)]$(PF_6)_2$ (**3**) at 30% probability level with partial numbering scheme. Counterions are omitted for clarity. Selected bond length data (Å): Co1-O1: 1.896(7), Co1-O2: 1.883(6), Co1-N1: 1.909(8), Co1-N2: 1.907(8), Co1-N3: 1.909(8), Co1-N4: 1.943(8).

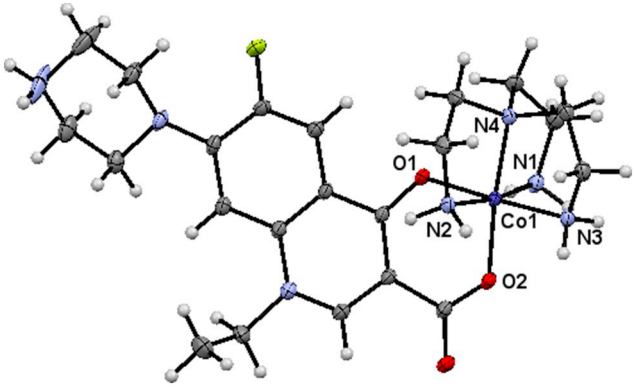

Fig. 8. ORTEP view of [Co(tpa)(nor)(Co(tpa)(norH)]$(PF_6)_3(Cl)_2{\cdot}5MeOH$ (**8**) at 50% probability level with partial numbering scheme, protonated at the piperazine nitrogen. Ordered and disordered counterions and solvent methanol molecules are omitted for clarity. Selected bond length data (Å): Co1-O1: 1.915(10), Co1-O2: 1.886(10), Co1-N1: 1.937(12), Co1-N2: 1.969(11), Co1-N3: 1.928(12), Co1-N4: 1.936(12).

3.1. Electrochemical studies

The reduction potential of cellular reductases is known to fall within the range −200 mV to −400 mV [44] (vs. NHE), while close to this lower limit or even a bit lower values have been determined in some hypoxic cells in a recent paper [45]. In order to explore the electrochemical properties and reduction potential values of the investigated Co(III) complexes, they were analysed by cyclic voltammetry, under the conditions given in the Experimental section. The results obtained were expected to provide information about the conditions under which the reduction of the complexes takes place and also whether these conditions allow the reduction by cellular reductases in normal or only in hypoxic tissues.

Based on the experimental findings, the following results were obtained:

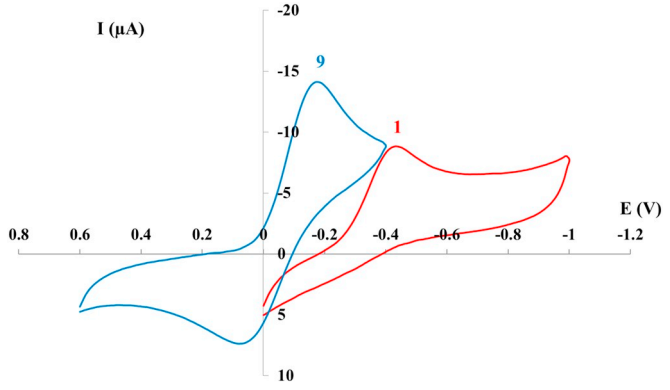

Fig. 9. CV curves registered for [Co(tpa)(lev)]$(ClO_4)_2$·3H_2O (**9**) and [Co(tren)(lev)]$(PF_6)_2$ (**1**) in water:MeOH = 1:1, referenced to Ag/AgCl electrode at a potential sweep rate of 200 mV/s and c = 1.0 mM.

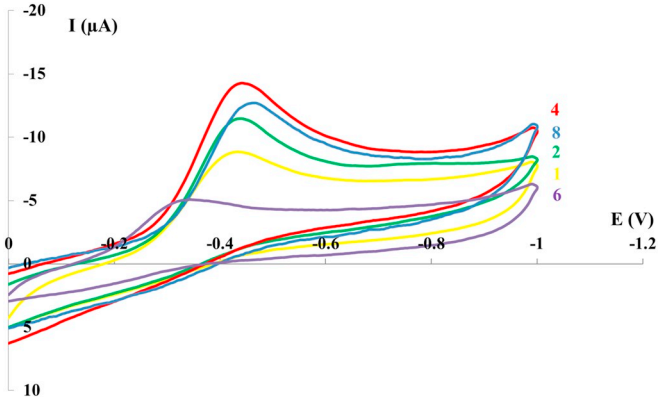

Fig. 10. CV curves registered for [Co(tren)(cip)]$(PF_6)_2$·1H_2O (**4**), [Co(tren)(nor)]$(PF_6)_2$ (**8**), [Co(tren)(nal)]$(PF_6)_2$ (**2**), [Co(tren)(lev)]$(PF_6)_2$ (**1**) and [Co(tren)(spa)]$(PF_6)(Cl)$·2H_2O (**6**) in water:MeOH = 1:1, referenced to Ag/AgCl electrode at a potential sweep rate of 200 mV/s and c = 1.0 mM.

(i). All of the studied complexes showed redox activity in the investigated voltage range. However, significant differences were obtained for the tren-containing complexes compared to the tpa analogs. While the cyclic voltammograms recorded for the former complexes showed irreversible reduction in accordance with earlier reports on [Co(tren)(O,O)] (O,O = hydroxamate) type complexes [46], the voltammograms indicated clearly the reversible redox processes of these novel tpa complexes. This is demonstrated in Fig. 9, where, for illustration, the voltammograms registered for [Co(tren)(lev)]$(PF_6)_2$ (**1**) and [Co(tpa)(lev)]$(ClO_4)_2$·3H_2O (**9**) are presented.

(ii). Fig. 9 also indicates that the reduction of the tren-containing complex happens at significantly lower voltage than the tpa-containing one.

(iii). The effect of the structural differences in the involved quinH ligands were investigated by comparison of the peak-potentials of the corresponding CV-curves. Small differences were obtained only in the case of tren-containing complexes. This is demonstrated in Fig. 10.

By evaluation of the voltammograms, the peak potentials, shown in Table 1, were obtained. The peak potentials measured against Ag/AgCl, were converted to NHE. The pK_a values of the bioligands also shown in Table 1 are taken from Ref. [47].

Based on Figs. 9 and 10 and also on results in Table 1, the following conclusions can be made:

1. Although previous investigations showed irreversible reduction of various ternary complexes formed either with Co(III)-tren or Co(III)-tpa in many cases [46], there are also examples for the above mentioned and illustrated (Fig. 9) differences between the reversibility of the redox reactions of the tren-containing complexes compared to the tpa-containing ones [22,48,49]. There is no doubt that these differences originate from the significant differences between the character of the 4N-donors of the two tripodal amines. While only σ-bonding is possible with the aliphatic-N atoms of tren, π-back-bonding interaction also occurs with the pyridyl-N atoms of tpa. This results in a decreased electron density at the central metal ion for the complexes of tpa compared to the corresponding tren-containing ones. This is the reason, why the cobalt(III) is significantly more reducible in the ternary complexes (the reduction potentials are less negative) with tpa versus tren. Moreover, the additional π-back-bonding interaction with tpa potentially results in decreased ligand lability, which might responsible for the significant differences between the reversibility of the reduction of the complexes with tren and tpa (the reduction of complexes of the former ligand completely irreversible in all investigated complexes, while reversible for the tpa-containing analogues).
2. The reduction potentials of the tren complexes are significantly more negative than those of the corresponding tpa analogues. This is in agreement with literature results [35] and again, can be assigned to the π-back-bonding capability of tpa as discussed above (point **1**.). Based on the reduction potential values, the tren complexes could be suitable for further examination as hypoxia-activated prodrugs.
3. The type of the quinH ligand has much less effect on the redox potential value of the complexes, than the type of the 4N donor ligand. The different substituents of the quinH ligands may be too far from the coordination center to cause larger change in the reducibility of the complex. A slight indication for some correlation between the basicity of the coordinating donor atom and the obtained peak potential might be assumed for the tren complexes (except spaH). Namely, parallel with the increase of the pK_a of quinH a slight decrease of the corresponding E_{pc} value is seen in Table 1.
4. Compared to the other complexes, a significantly less negative E_{pc} was determined for the spa-containing one, [Co(tren)(spa)]$(PF_6)(Cl)$·2H_2O. Because ^{19}F NMR measurements supported the same coordination mode in this complex as it is in all the others (see above), the difference is assumed to be caused by the electronic effect of –NH_2 group, being close enough to the coordinating atom to indicate this change in the E_{pc} value.

3.2. Biological studies

The effect of **4** and **5** on human cancer and noncancerous cells was tested using MTT assay. Human breast adenocarcinoma MCF-7 cells, human cervical carcinoma HeLa cells, breast carcinoma MDA-MB-231 cells and human MRC-5 pd30 cells (derived from normal lung tissue) were incubated with the Co(III) complexes, and metabolic activity in cell cultures was evaluated as described in the Experimental section. The IC_{50} values determined for 72 h of the treatment are reported in Table 2. Both ternary cobalt complexes showed very low antiproliferative activity towards both cancer and noncancerous cells (the Co-complexes without ciprofloxacin were even much less active then compounds **4** and **5**). Similarly, free ciprofloxacin also showed a very low effect in human cells, in agreement with already published data, where significant cytotoxic effect of cipH was shown at the concentration of 200–500 mg/mL (0.6–1.5 mM) [50,51]. Low toxic effects towards human cells is a prerequisite for a safe application of ciprofloxacin as antimicrobial agent.

Ciprofloxacin is a well-known antibiotic and since 1987, when introduced into the medical practice, is widely used to treat a number of

Table 1
Catodic (E_{pc}) and anodic (E_{pa}) peak potential values (mV) of the $[Co(4N)(quin)]^{2+}$ (4N = tren or tpa) complexes against NHE together with the pK_a values of the quinH ligands.

quinH	levH		nalH		cipH		norH		spaH	
pK_a	5.50		5.95		6.09		6.34		6.25	
E (mV), H_2/H^+	E_{pc}	E_{pa}	E_{pc}	E_{pa}	E_{pc}	E_{pa}	E_{pc}	E_{pa}	E_{pc}	E_{pa}
tren	−222	–	−231	–	−242	–	−252	–	−133	–
tpa	+35	+288	+61	+309	+31	+329	+35	+292	–	–

Table 2
IC_{50} mean values[a] (μM) obtained for **4**, **5**, cipH, $[Co(tren)Cl_2]Cl$ and $[Co(tpa)Cl_2]Cl$ (after 72 h of incubation) by MTT assay.

	HeLa	MCF 7	MDA-MB-239	MRC5 pd30
4	> 250	> 250	> 250	> 250
5	230 ± 25	220 ± 18	258 ± 30	> 300
cipH	270 ± 10	n.d.	407 ± 12	> 500
$[Co(tren)Cl_2]Cl$	> 2000	> 2000	1380 ± 330	> 2000
$[Co(tpa)Cl_2]Cl$	1340 ± 310	1660 ± 300	1010 ± 280	1820 ± 420

[a] Data represent a mean ± SD from at least three independent experiments, each of them made in triplicate.

bacterial infections [52]. The mechanism of antibacterial action of ciprofloxacin (and other quinolones) consists of inhibition of DNA gyrase and DNA topoisomerase IV that control DNA topology and are essential for bacterial replication [53,54]. Quinolones intercalate into the DNA and interact with the protein at the enzyme−DNA interface, acting as physical blocks to enzyme action [54]. Therefore, the effects of the two selected complexes, **4** and **5**, bearing cipH on bacterial growth and DNA gyrase activity were investigated along with their DNA interactions.

To assess an antibacterial effect of **4** and **5**, the bacterial strain K-12 of *E. coli* was used as a model organism and the minimum inhibitory concentrations were determined after 24 h incubation. As shown in Fig. 11, both complexes were able to reduce bacterial growth even in the initial stage of the experiment, with **5** being more efficient than **4**. However, both Co(III) complexes were less active than the free ciprofloxacin. Minimum inhibitory concentrations determined after 24 h of incubation with bacterial suspension were 6.12, 2.18, and 1.47 μM for **4**, **5** and cipH, respectively.

To examine whether the antibacterial activity of **4** and **5** is related to inhibition of DNA-gyrase (similarly as that of free ciprofoxacin), decatenation - supercoiling assay was employed. The method is based upon detection of kinetoplast DNA (kDNA) that can be negatively supercoiled by DNA gyrase. As indicated in Fig. 12, both Co-complexes were able to inhibit bacterial DNA gyrase with **5** being slightly more inhibitory than **4**.

The DNA-gyrase inhibition of ciprofloxacin is closely related to its ability to intercalate into DNA and form DNA-protein complex [55]. Thus, the interactions of the complexes **4** and **5** with DNA were also studied by various techniques in order to explore the extent and type of DNA interaction.

First, the changes occurring in UV–Vis absorption spectra of the Co (III) complexes following the addition of ct DNA were investigated. The absorption spectra of **4** and **5** displayed an absorption band in the region of 310–400 nm (Fig. S2). This allowed us to monitor the spectral changes in this region resulting from DNA interaction without interference from DNA absorption. The absorption spectra of **4** and **5** in the presence of a gradually increasing concentration of ct DNA are shown in Fig. 13. The data reveal a decrease in maximal intensities (hypochromism ca. 35 and 30% for of **4** and **5**, respectively) and a slight bathochromic shift to higher wavelengths. It is widely accepted that hypochromism and, particularly, bathochromic shifts are often associated with the intercalation mode of DNA interaction with low molecular mass compounds as a result of strong stacking interactions between DNA base pairs and the aromatic chromophore of the cip ligand. Thus, the results are indicative of interaction of both Co-complexes with ct DNA.

The binding constants (K) of the complexes **4** and **5** to ct DNA were calculated using the McGhee and von Hippel plots [56]. The binding constants found in this way were 6.3×10^4 and 11.9×10^4 for **4** and **5**, respectively, values that roughly correspond to the typical binding constants for intercalators (10^5–10^9). The larger *K* value for **5** may indicate the role of the pyridyl units of tpa in DNA binding of this complex too. In contrast, the binding constants of the groove binders are usually higher, ca. 10^9–10^{11} [57].

Flow LD is also sensitive to interactions between DNA and small molecules. Therefore LD spectra of ct DNA were acquired in the absence or presence of the increasing concentrations of **4** and **5** in 0.01 M Tris.Cl, pH 7.4 (Fig. 14A,B). The helical axis of DNA orients along the

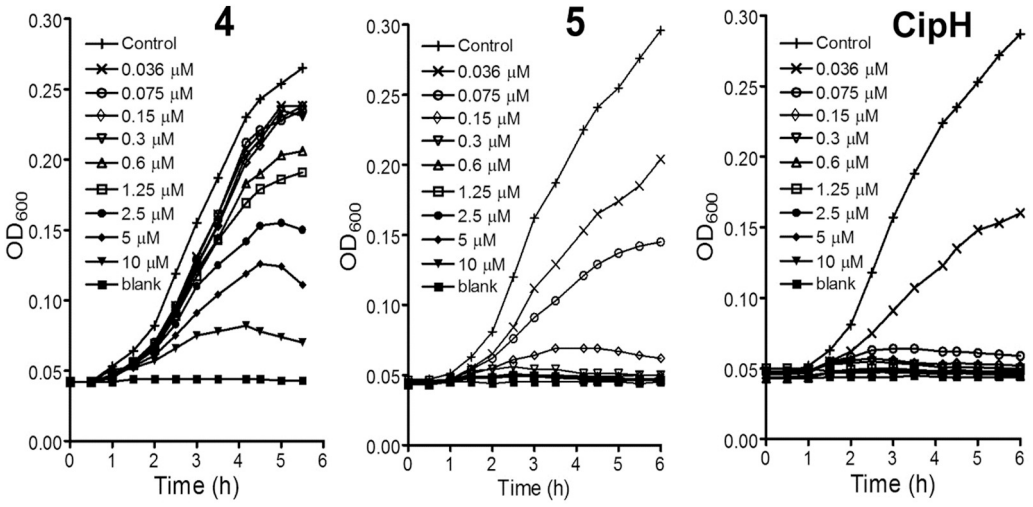

Fig. 11. The effect of various concentrations of **4** (left), **5** (middle), and cipH (right) on K-12 *E. coli* growth. The data are taken from one representative run.

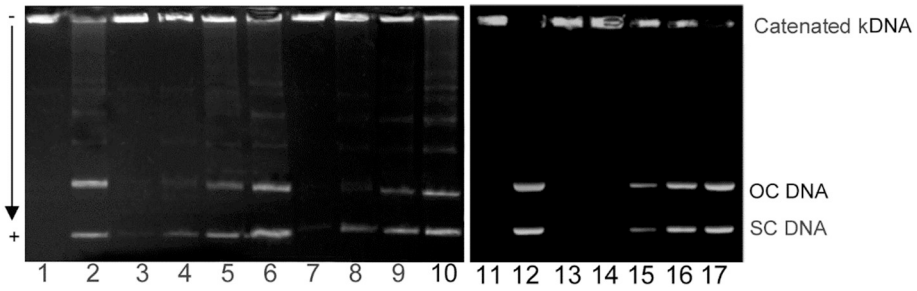

Fig. 12. Effect of **4** and **5** on DNA decatenation by bacterial DNA gyrase. kDNA (0.4 μg) was incubated with the enzyme in the absence or presence of the complexes at various concentrations. DNA products were separated by agarose gel electrophoresis. Lanes 1 and 11, kDNA; lanes 2 and 12, kDNA plus gyrase in the absence of drug; lanes 3, 4, 5, and 6, kDNA plus gyrase in the presence of 120, 90, 60 and 30 μM complex **4**, respectively; lanes 7, 8, 9 and 10, kDNA plus gyrase in the presence of 120, 90, 60 and 30 μM complex **5**, respectively; lanes 13, 14, 15, 16, and 17, kDNA plus gyrase in the presence of 60, 30, 15, 7, and 3 μM cipH, respectively.

flow axis. Since the base pairs are oriented perpendicularly to the DNA helix axis, the π-π transitions in the B-DNA base pairs, therefore, result in a negative LD signal in the 240–280 nm region. Free, unbound molecules of **4** and **5** are too small to be orientated in the experiment and therefore showed no signal. Thus, the LD signals in the region of absorption of the Co complexes (310–400 nm) that arise after DNA interaction prove unequivocally that the complexes bind to DNA in specific, non-random orientations. The negative orientation of LD signals in the region of 310–400 nm also suggests that the angle of the long axis of **4** and **5** to the axis of the DNA double helix is > 54°, as would be expected for an intercalator [58]. The negative DNA LD bands in the range 240–280 nm confirm that the DNA in the presence of the Co complexes remains in the B-DNA conformation.

A key feature of the classic intercalation model is the lengthening of the DNA helix as the base pairs are separated to accommodate the ligand. Thus, the intercalators dramatically increase the length of DNA, in contrast to the groove binders that do not lengthen the DNA helix. Therefore, hydrodynamic methods sensitive to length changes (sedimentation or viscosity) have been among the most stringent tests of the binding mode of DNA binding agents [59]. The results of the viscosity measurements of DNA modified with **4** or **5** are shown in Fig. 14C. The interaction of DNA with these Co(III) complexes results in an increase of relative viscosity of DNA, indicating lengthening of the DNA helix, in agreement with intercalative binding mode of complexes.

The interaction of small molecules with DNA can influence its melting temperature. Binding of compounds to DNA by an intercalation stabilizes the double helical structure, thus increasing the T_m of the ligand–DNA complex. Therefore, the effect of **4** and **5** on thermal stability of DNA was also assessed. As indicated in Figs. 14D and S3, both complexes markedly increased the melting temperature of DNA under the experimental conditions used. Such substantial potency of both Co-complexes to affect the thermal stability of DNA further supports the view that they bind DNA by an intercalative mode.

In order to obtain information on the ability of **4** and **5** to cleave DNA, native agarose gel electrophoresis was also carried out. This assay monitors the extent of single strand breaks in DNA as a function of the conversion of supercoiled pBR322 DNA into nicked form (OC). As shown in Fig. S4, there were no significant changes in the intensities of particular bands related to the supercoiled (SC) and nicked/open circular (OC) form after 45 min of incubation, indicating no DNA degradation due to the strand cleavage, in contrast to the effect already described for some cobalt(II) complexes with ciprofloxacin [17].

4. Conclusions

Five quinolones, nalidixic acid (nalH), and its four fluoro derivatives, ciprofloxacin (cipH), norfloxacin (norH), sparfloxacin (spaH) and levofloxacin (levH) were used to synthesize novel cobalt(III) ternary complexes bearing 4N donor ligands (tris(2-aminoethyl)amine (tren) or tris(2-methylpyridyl)amine (tpa)) to stabilize the 3+ oxidation state of the metal ion.

In all of the complexes (O,O) coordination mode of the quinolones was found by ^{1}H NMR. This was also supported by X-ray in two cases, [Co(tpa)(nal)](PF$_6$)$_2$ and [Co(tpa)(nor)(Co(tpa)(norH)](PF$_6$)$_3$(Cl)$_2$·5MeOH. For spaH, the involvement of the amino moiety, which is in chelatable position to the oxo group, was ruled out in the

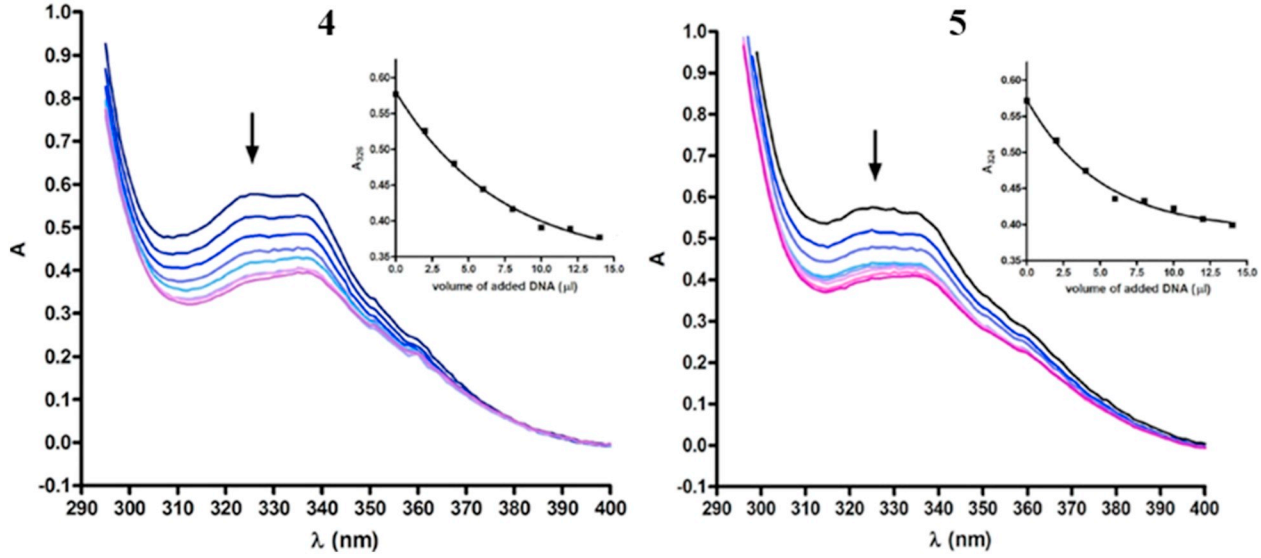

Fig. 13. UV–Vis absorption spectra of **4** (left) and **5** (right) at 5.3 × 10^{-5} M concentration in the absence (upper line) or in the presence of increasing concentrations of ct DNA in 0.01 M Tris.Cl buffer (pH 7.4; 24 °C). The arrows indicate the absorption change upon increasing amount of ct DNA. Insert graphs show the plot of absorbance at λ_{max} versus the amount of DNA added to the samples.

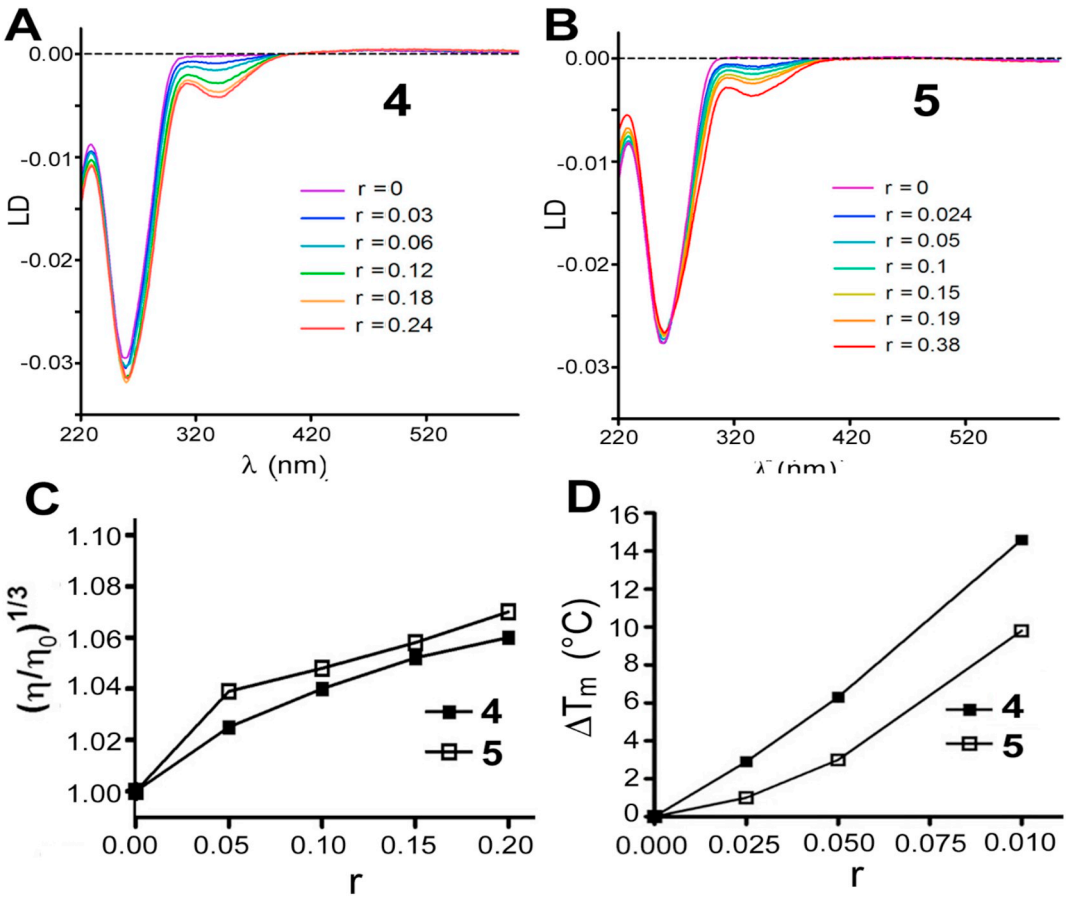

Fig. 14. A, B: Linear dichroism spectra of ct DNA (0.2 mM) in the absence or presence of increasing concentrations of **4** (A) and **5** (B) in 0.01 M Tris-Cl, pH 7.4. C: Dependence of relative viscosity of ct DNA after their interaction with **4** (full symbols) or **5** (open symbols) on r. The data were measured for DNA concentration of 0.15 mg/mL (4.7×10^{-4} M, related to the monomer content) in 0.01 M Tris-Cl, pH 7.4. D: Plots showing the dependence of ΔT_m values on r for ct DNA modified by **4** (full symbols) and **5** (open symbols). The melting curves were recorded in 0.01 M Tris-Cl, pH 7.4. ΔT_m is defined as the difference between the T_m values of the modified and unmodified DNA. Data measured in triplicate varied on average by 2% from their mean. In all panels, r is defined as a molar ratio of Co-complex to DNA (in bases) (r = [complex]/[DNA]).

coordination by ^{19}F NMR.

One of the aims of the work was to create a new series of inert Co(III) complexes which might be able to transport a quinolone in its inactivated (coordinated) form to a target in hypoxic area and releasing it there via dissociation, following the reduction of the central Co(III) to Co(II). Consequently, investigation of the redox character of the complexes was part of this work and based on the results the following conclusions could be made. (i) No significant systematic change in the redox behaviour upon changing the quinolone in the complexes was detected, except for the ternary complex formed between Co(III)-tren and sparH, where, compared to the others, the electronic effect of the amino moiety caused a ca. 100 mV increase in the reduction potential, E_{pc}. (ii) The different character of the two 4N-donor ligands, however, resulted in very different redox behavior of the complexes formed with them. Namely, the π-back-bonding interaction with tpa, compared to the corresponding complexes with tren, caused a measurable increase in the redox potential (the E_{pc} values are ca. +35 mV with tpa, while fell into the range −220 to −250 mV with tren), as well as a significant increase in the ligand lability (the reduction of the tren-containing complexes is irreversible under the investigated conditions, while reversible for the tpa analogues). Accordingly, the relatively high redox potential values determined for the tpa-containing complexes suggest the ability of them to get reduced even under normoxic conditions, moreover, the reversibility of their redox processes shows that reoxidation of the central metal ion can easily happen. As a consequence, the obtained electrochemical results indicate that the Co(III)-tpa-quinolone complexes are not good candidates for the development of effective, highly selective hypoxia-activated pro-drug complexes, but this might be achieved by substitution of tpa by tren.

The results of biological studies show relatively low toxic effect of both **4** and **5** in human cells. In contrast, they showed relatively good antimicrobial activity, with MIC in a micromolar range of concentrations. The significantly higher (ca 100-times) toxicity of **4** and **5** to the bacterial over the human cells represents a potential for development of new antibacterial drugs. Nevertheless, the potency of the compounds to other then *E. coli* bacteria including the resistant strains still needs to be tested. The decatenation assay also revealed that inhibition of bacterial DNA–gyrase plays an important role in the mechanism of action of both **4** and **5**, similarly as in the case of free ciprofloxacin. Both complexes also intercalate to DNA, as confirmed by the increase of relative viscosity and melting temperature of DNA, and also by induction of negative LD signal in the region of absorption of both complexes as a consequence of interaction of **4** or **5** with double-helical DNA.

Acknowledgement

The research was supported by the EU and co-financed by the European Regional Development Fund under the projects GINOP-2.3.2-15-2016-00008, GINOP-2.3.3-15-2016-00004 and the Hungarian Scientific Research Fund (OTKA K112317). JK and HS acknowledge the support from the Palacky University project IGA PrF 2018 022. The work of VB was supported by the Czech Science Foundation (Grant 18-095025).

Appendix A. Supplementary data

Supplementary data to this article can be found online at https://doi.org/10.1016/j.jinorgbio.2019.01.005.

References

[1] P.C. Appelbaum, P.A. Hunter, Int. J. Antimicrob. Agents 16 (2000) 5–15.
[2] L.A. Mitschel, Chem. Rev. 105 (2005) 559–592.
[3] A. Mustaev, M. Malik, X. Zhao, N. Kurepina, G. Luan, L.M. Oppegard, H. Hiasa, K.R. Marks, R.J. Kerns, J.M. Berger, K. Drlica, J. Biol. Chem. 289 (2014) 12300–12312.
[4] M.I. Andersson, A.P. MacGowan, J. Antimicrob. Chemother. 51 (2003) 1–11.
[5] A.M. Emmerson, A.M. Jones, J. Antimicrob. Chemother. 51 (2003) 13–20.
[6] I. Laponogov, X.S. Pan, D.A. Veselkov, R.T. Cirz, A. Wagman, H.E. Moser, L.M. Fisher, M.R. Sanderson, Open Biol. 6 (2016) 160157.
[7] V. Uivarosi, Molecules 18 (2013) 11153–11197.
[8] I. Turel, Coord. Chem. Rev. 232 (2002) 27–47.
[9] M.J. Feio, I. Sousa, M. Ferreira, L. Cunha-Silva, R.G. Saraiva, C. Queirós, J.G. Alexandre, V. Claro, A. Mendes, R. Ortiz, S. Lopes, A.L. Amaral, J. Linoa, P. Fernandes, A.J. Silva, L. Moutinho, B. de Castro, E. Pereira, L. Perelló, P. Gameiro, J. Inorg. Biochem. 138 (2014) 129–143.
[10] M.S. Refat, Spectrochim. Acta A 68 (2007) 1393–1405.
[11] C. Protogeraki, E.G. Andreadou, F. Perdih, I. Turel, A.A. Pantazaki, G. Psomas, Eur. J. Med. Chem. 86 (2014) 189–201.
[12] R. Koziel, J. Szczepanowska, A. Magalska, K. Piwocka, J. Duszynski, K. Zablocki, J. Physiol. Pharmacol. 61 (2) (2010) 233–239.
[13] O. Aranha, D.P. Wood Jr., F.H. Sarkar, Clin. Cancer Res. 6 (2000) 891–900.
[14] A.M. Kamat, D.L. Lamm, Urology 63 (3) (2004) 457–460.
[15] N. Gurtowska, T. Kloskowski, T. Drewa, Med. Sci. Monit. 16 (10) (2010) 218–223.
[16] M.N. Patel, M.R. Chhasatia, D.S. Gandhi, Bioorg. Med. Chem. Lett. 19 (2009) 2870–2873.
[17] M.N. Patel, M.R. Chhasatia, B. Bhatt, Med. Chem. Res. 20 (2011) 220–230.
[18] I. Tsitsa, A. Tarushi, P. Doukoume, F. Perdih, A. de Almeida, A. Papadopoulos, S. Kalogiannis, A. Casini, I. Turel, G. Psomas, RSC Adv. 6 (2016) 19555–19570.
[19] Y. Xia, Z.Y. Yang, S.L. Morris-Natschke, K.H. Lee, Curr. Med. Chem. 6 (3) (1999) 179–194.
[20] T.W. Failes, C. Cullinane, C.I. Diakos, N. Yamamoto, J.G. Lyons, T.W. Hambley, Chem. Eur. J. 13 (2007) 2974–2982.
[21] T.W. Failes, T.W. Hambley, Dalton Trans. (2006) 1895–1901.
[22] P.D. Bonnitcha, B.J. Kim, R. Hocking, J.K. Clegg, P. Turner, S.M. Neville, T.W. Hambley, Dalton Trans. 41 (2012) 11293–11304.
[23] D.C. Ware, P.J. Brothers, G.R. Clark, W.A. Denny, B.D. Palmer, W.R. Wilson, J. Chem. Soc. Dalton Trans. (2000) 925–932.
[24] Z. Tyeklár, R.R. Jacobson, N. Wei, N.N. Murthy, J. Zubieta, K.D. Karlin, J. Am. Chem. Soc. 115 (1993) 2611–2689.
[25] E. Kimura, S. Young, J.P. Collman, Inorg. Chem. 9 (5) (1970) 1183–1191.
[26] G.M. Sheldrick, Acta Cryst A64 (2008) 112–122.
[27] L.J. Farrugia, J. Appl. Crystallogr. 32 (1999) 837–838.
[28] S.P. Westrip, J. Appl. Crystallogr. 43 (2010) 920–925.
[29] A.L. Spek, J. Appl. Crystallogr. 36 (2003) 7–13.
[30] E. Farkas, P. Buglyó, É.A. Enyedy, M.A. Santos, Inorg. Chim. Acta 357 (2004) 2451–2461.
[31] R.J.W. Lambert, J. Pearson, J. Appl. Microbiol. 88 (5) (2000) 784–790.
[32] S. Lecomte, M.H. Baron, M.T. Chenon, C. Coupry, N.J. Moreau, Antimicrob. Agents Chemother. 38 (1994) 2810–2816.
[33] E.K. Efthimiadou, A. Karaliota, G. Psomas, Bioorg. Med. Chem. Lett. 18 (2008) 4033–4037.
[34] E. Kouris, S. Kalogiannis, F. Perdih, I. Turel, G. Psomas, J. Inorg. Biochem. 163 (2016) 18–27.
[35] Z.H. Chohan, C.L. Supuran, A. Scozzafava, J. Enzyme Inhib. Med. Chem. 20 (3) (2005) 303–307.
[36] F.A.I. Al-Khodir, M.S. Refat, Russ. J. Gen. Chem. 85 (2015) 718–730.
[37] S.A. Sadeek, J. Mol. Struct. 753 (2005) 1–12.
[38] F.A.I. Al-Khodir, M.S. Refat, J. Mol. Struct. 1094 (~~15~~) (2015) 22–35.
[39] Z. An, J. Huang, W. Qi, Acta Cryst E63 (2007) m2009.
[40] W.Y. Huang, J. Li, S.L. Kong, Z.C. Wang, H.L. Zhu, RSC Adv. 4 (2014) 35193–35204.
[41] J.H. He, D.R. Xiao, H.Y. Chen, D.Z. Sun, S.W. Yan, X. Wang, Z.L. Ye, Q.L. Luo, E.B. Wang, J. Solid State Chem. 198 (2013) 279–288.
[42] S. Wang, J. Qin, X.L. Wang, C. Qin, T.T. Li, Z.M. Su, CrystEngComm 13 (2011) 325–329.
[43] Z. An, W. Xu, R.S. Wang, Acta Cryst E63 (2007) m507–m508.
[44] D.C. Ware, B.D. Palmer, W.R. Wilson, W.A. Denny, J. Med. Chem. 36 (1993) 1839–1846.
[45] J. Jiang, C. Auchinvole, K. Fischer, C.J. Cambell, Nanoscale 6 (2014) 12104–12110.
[46] P. Buglyó, I. Kacsir, M. Kozsup, I. Nagy, S. Nagy, A.C. Bényei, E. Kovats, E. Farkas, Inorg. Chim. Acta 472 (2018) 234–242.
[47] P. Pawar, R. Katara, S. Mishra, D.K. Majumdar, Expert Opin. Drug Deliv. 10 (5) (2013) 691–711.
[48] M. Yano, M. Fujita, M. Miyake, M. Tatsumi, T. Yajima, O. Yamauchi, M. Oyama, K. Sato, T. Takui, Polyhedron 26 (2007) 2174–2178.
[49] Y. Suenaga, H. Inada, M. Inomata, R. Yamaguchi, I. Okubo, M. Maekawa, T. Kuroda-Sowa, Chem. Lett. 43 (2014) 562–564.
[50] C. Herold, M. Ocker, M. Ganslmayer, H. Gerauer, E.G. Hahn, D. Schuppan, Br. J. Cancer 86 (2002) 443–448.
[51] A. Gurbay, B. Gonthier, L. Barret, A. Favier, F. Hincal, Toxicology 229 (2007) 54–61.
[52] E. Torok, Ed Moran, F. Cooke, Oxford Handbook of Infectious Diseases and Microbiology, OUP Oxford, 2009, p. 56 (ISBN 978-0-19-103962-1).
[53] E. Pestova, J.J. Millichap, G.A. Noskin, L.R. Peterson, Antimicrob. Agents Chemother. 45 (2000) 583–590.
[54] Y. Pommier, E. Leo, H. Zhang, C. Marchand, Chem. Biol. 17 (2010) 421–433.
[55] Z. Katie, J. Aldred, R.J. Kerns, N. Osheroff, Biochemistry 53 (2014) 1565–1574.
[56] J.D. McGhee, P.H. von Hippel, J. Mol. Biol. 86 (1974) 469–489.
[57] J.B. Chaires, Biopolymers 44 (1997) 201–215.
[58] A. Rodger, R. Marington, M.A. Geeves, M. Hicks, L. de Alwis, D.J. Halsall, T.R. Dafforn, Phys. Chem. Chem. Phys. 8 (2006) 3161–3171.
[59] S. Satyanarayana, J.C. Dabrowiak, J.B. Chaires, Biochemistry 32 (1993) 2573–2584.